

# Defect Characteristics of Reverse Hill-Sachs Lesions

Philipp Moroder,<sup>\*†</sup> MD, Mark Tauber,<sup>†‡</sup> MD, Markus Scheibel,<sup>§</sup> MD, Peter Habermeyer,<sup>‡</sup> MD, Andreas B. Imhoff,<sup>||</sup> MD, Dennis Liem,<sup>¶</sup> MD, Helmut Lill,<sup>#</sup> MD, Stefan Buchmann,<sup>||</sup> MD, Julia Wolke,<sup>§</sup> MD, Alberto Guevara-Alvarez,<sup>||</sup> MD, Katharina Salmoukas,<sup>#</sup> MD, and Herbert Resch,<sup>†</sup> MD

*Investigation performed by the German Society for Shoulder and Elbow Surgery (DVSE)*

**Background:** Little scientific evidence regarding reverse Hill-Sachs lesions (RHSLs) in posterior shoulder instability exists. Recently, standardized measurement methods of the size and localization were introduced, and the biomechanical effect of the extent and position of the defects on the risk of re-engagement was determined.

**Purpose:** To analyze the characteristics and patterns of RHSLs in a large case series using standardized measurements and to interpret the results based on the newly available biomechanical findings.

**Study Design:** Case series; Level of evidence, 4.

**Methods:** In this multicenter study, 102 cases of RHSLs in 99 patients were collected from 7 different shoulder centers between 2004 and 2013. Patient- as well as injury-specific information was gathered, and defect characteristics in terms of the size, localization, and depth index were determined on computed tomography or magnetic resonance imaging scans by means of standardized measurements. Additionally, the position (gamma angle) of the posterior defect margin as a predictor of re-engagement was analyzed.

**Results:** Three types of an RHSL were distinguished based on the pathogenesis and chronicity of the lesion: dislocation (D), locked dislocation (LD), and chronic locked dislocation (CLD). While the localization of the defects did not vary significantly between the subgroups ( $P = .072$ ), their mean size differed significantly (D:  $32.6^\circ \pm 11.7^\circ$ , LD:  $49.4^\circ \pm 17.2^\circ$ , CLD:  $64.1^\circ \pm 20.7^\circ$ ;  $P < .001$ ). The mean gamma angle as a predictor of re-engagement was similarly significantly different between groups (D:  $83.8^\circ \pm 14.5^\circ$ , LD:  $96.5^\circ \pm 17.9^\circ$ , CLD:  $108.7^\circ \pm 18.4^\circ$ ;  $P < .001$ ). The orientation of the posterior defect margin was consistently quite parallel to the humeral shaft axis, with a mean difference of  $0.3^\circ \pm 8.1^\circ$ .

**Conclusion:** The distinction between the 3 different RHSL types based on the pathogenesis and chronicity of the defect helps identify defects prone to re-engagement. The gamma angle as a measurement of the position of the posterior defect margin and therefore a predictor of re-engagement varies significantly between the defect types.

**Keywords:** reverse Hill-Sachs lesion; posterior shoulder instability; posterior shoulder dislocation; locked dislocation; chronic locked dislocation; gamma angle

\*Address correspondence to Philipp Moroder, MD, Department of Traumatology and Sports Injuries, Paracelsus Medical University, Muellner Hauptstrasse 48, 5020 Salzburg, Austria (email: philipp.moroder@pmu.ac.at).

†Department of Traumatology and Sports Injuries, Paracelsus Medical University, Salzburg, Austria.

‡Department of Shoulder and Elbow Surgery, ATOS Clinic Munich, Munich, Germany.

§Center for Musculoskeletal Surgery, Charité-Universitätsmedizin Berlin, Berlin, Germany.

||Department for Orthopaedic Sports Medicine, Technical University Munich, Munich, Germany.

¶Department of Orthopedics and Tumor Orthopedics, University Hospital Muenster, Muenster, Germany.

#Department of Trauma and Reconstructive Surgery, Friederikenstift Hospital Hanover, Hanover, Germany.

The authors declared that they have no conflicts of interest in the authorship and publication of this contribution.

Posterior shoulder dislocations are often accompanied by an anteromedial humeral head impression fracture that, depending on the type of instability and especially the type of employed imaging modality (radiography, computed tomography [CT], or magnetic resonance imaging [MRI]), can be observed in 30% to 90% of the cases.<sup>12,14</sup> This impression fracture is commonly known as a reverse Hill-Sachs lesion (RHSL) in analogy to the Hill-Sachs lesion encountered in anterior shoulder instability.<sup>7</sup> RHSLs are also called Malgaigne lesions because the first description of humeral head defects caused by shoulder instability in general has been attributed to the 19th century French surgeon Joseph-Francois Malgaigne. The pathogenesis of an RHSL is the impaction of the posterior glenoid rim into the anteromedial humeral articular surface during a posterior shoulder dislocation or subluxation. Because of recurrent engagement with the posterior

glenoid rim, an RHSL can result in chronic posterior shoulder instability and additionally might represent a risk factor for early-onset osteoarthritis because of contact of the partially destructed humeral articular surface with the glenoid.<sup>8,9</sup> Currently, the treatment of RHSLs is mainly determined by the defect extent, with recommendations being based on small case series or expert opinions and therefore remaining under debate.<sup>2,8,11</sup> Moreover, all current treatment recommendations rely on the mere estimation of the defect size, which proved unreliable in a recent study, which in turn leads to the assumption that the choice of treatment in general lacks reproducible scientific evidence.<sup>10</sup> In an attempt to improve the scientific evidence on the subject, a standardized measurement technique to quantify the extent and also the localization of RHSLs has been introduced and its reliability proven.<sup>10</sup> In a biomechanical analysis, it has been shown that indeed not only the size of the defect is predictive for re-engagement with the posterior glenoid rim but also its localization. A combined measurement of size and localization (the “gamma angle”) was introduced to identify defects prone to re-engagement.<sup>9</sup>

However, the clinical implications of these new findings are yet to be determined. In a multicenter study, a large variety of CT and MRI data sets of patients who experienced a single episode or multiple episodes of posterior shoulder instability with sustained RHSLs was gathered, and the observed defects were analyzed along with patient- and injury-specific information. The goal of this study was to determine the pathomorphological characteristics and patterns of RHSLs in patients after a posterior shoulder dislocation.

## METHODS

In this multicenter retrospective study from the German Society for Shoulder and Elbow Surgery (Deutsche Vereinigung für Schulter- und Ellenbogenchirurgie [DVSE]), data from 7 affiliated high-volume shoulder centers were collected. Included were all patients (1) who experienced an episode of posterior shoulder instability (acute or chronic, first time or recurrent), (2) with a concomitant humeral head impression fracture (simple impression, head-split fractures, concomitant fractures of the proximal humerus), and (3) who had received a CT or MRI scan with at least an axial and coronal plane reconstruction on admission between 2004 and 2013 regardless of the ensuing type of treatment. Ethical committee approval was obtained for this study before its beginning.

All institutions retrospectively collected anonymized CT and MRI data sets of included patients, which were then pooled and analyzed for defect characteristics using the imaging software Impax EE R20 VIII (Agfa HealthCare). Measurements included the defect extent (alpha angle), localization (beta angle), and a combined measurement identifying the position of the posterior defect margin (gamma angle) as described by Moroder et al.<sup>10</sup> (Figure 1). The depth index was determined by calculating the ratio between the depth of the defect and the diameter of a best-fit circle placed on the humeral articular surface

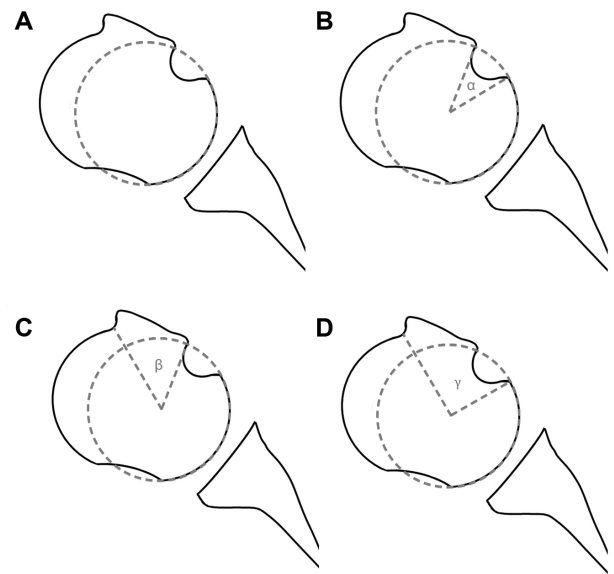


**Figure 1.** Measurements of reverse Hill-Sachs lesions were performed according to Moroder et al.<sup>10</sup> (A) A best-fit circle was placed over the remainder of the humeral articular surface, and (B) lines were drawn from the defect edges to the center of the circle, creating an angle (alpha) that describes the defect extent. (C) The localization of the defects was determined by measuring the angle (beta) between the anterior edge of the defect and the bicipital sulcus. (D) The summation of the alpha and beta angles results in the gamma angle, which describes the angle between the posterior defect edge and the bicipital sulcus.

as detailed by Moroder et al.<sup>10</sup> Image analysis was performed by the first author (P.M.) as a center-independent observer. The reliability of the described angle measurements has been proven in a previous study.<sup>10</sup> Additionally, images were analyzed for fractures of the tuberosities, surgical neck fractures, head-split components, as well as posterior glenoid rim defects. When CT scans were available, a 3-dimensional (3D) reconstruction was performed using image processing software (OsiriX; Pixmeo Sarl), and the orientation of the posterior edge of the defect in relation to the humeral shaft axis was analyzed (Figure 2). In the case of available MRI scans, an additional evaluation of the capsulolabral complex, the biceps tendon, and the rotator cuff was carried out.

Additionally, all institutions provided anonymized information about the patients' age, sex, affected side, handedness, type of instability event (locked, dislocated with subsequent reduction, subluxation), chronicity, number of dislocations, cause of primary dislocation, cause of last dislocation, time elapsed since first dislocation, time elapsed since last dislocation, concomitant shoulder injuries, treatment type, multidirectional instability assessed by clinical testing, instability of contralateral side, generalized joint hyperlaxity, and eventual previous surgical treatment.

All patients were divided into 3 groups based on the pathogenesis and chronicity of their RHSL: (1) posterior

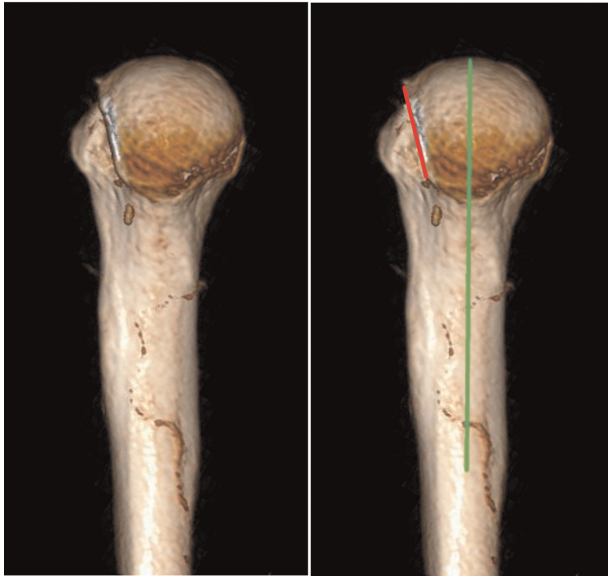


**Figure 2.** Orientation of the posterior defect edge of reverse Hill-Sachs lesions (red line) was measured on 3-dimensional reconstructions of computed tomography scans in relation to the humeral shaft axis (green line).

shoulder dislocation (group D), (2) locked posterior shoulder dislocation (group LD), and (3) chronic locked posterior shoulder dislocation (group CLD).

A dislocation was defined as an instability episode without persisting engagement of the RHSL with the posterior glenoid rim. A locked dislocation was defined as an instability event with persisting engagement of the RHSL, necessitating manual or surgical reduction. A chronic locked dislocation was defined as a locked dislocation persisting for at least 3 weeks before hospital admission.<sup>13</sup> A tuberosity fracture was considered to be displaced if the displacement was greater than 5 mm.<sup>1,5</sup>

### Statistical Analysis

All variables were tested for normal distribution. For parametric statistical comparison between independent samples, an analysis of variance with post hoc testing (Bonferroni) was performed. For nonparametric statistical analysis of independent samples, a Kruskal-Wallis or Mann-Whitney *U* test was employed. For nominal data comparison, the  $\chi^2$  test was utilized. A Pearson correlation coefficient was calculated for the comparison between CT and MRI measurements of the alpha angle, beta angle, gamma angle, and depth index in the 10 cases in which both imaging methods were available. For all tests, the  $\alpha$  level was set to .05.

## RESULTS

A total of 102 cases of RHSLs in 99 patients were collected from 7 different shoulder departments. According to the previously mentioned classification criteria, 34 cases

were allocated to group D, 58 cases to group LD, and 10 cases to group CLD. Patient characteristics and group comparisons are displayed in Table 1. Causes for instability episodes in the 3 different groups are listed in Table 2. CT scans were available for 62 cases, MRI scans were available for 30 cases, and both CT and MRI scans were available for 10 cases.

A statistically significant difference between the 3 groups regarding the alpha angle (defect size) and gamma angle (position of the posterior defect margin) was observed (both  $P < .001$ ). No statistical difference in the beta angle (defect localization) could be identified ( $P = .072$ ) (Figure 3). The depth index of the RHSLs showed statistically significant differences between all groups ( $P < .001$ ) (Figure 4).

A comparison of the CT and MRI measurements for the alpha angle, beta angle, gamma angle, and depth index in the 10 cases in which both imaging modalities were available revealed a correlation coefficient of 0.975, 0.915, 0.903, and 0.961, respectively. The mean measurement difference for the alpha angle, beta angle, and gamma angle was below 5°, and the mean measurement difference for the depth index was below 1%. Twelve cases of the LD group and 2 cases of the CLD group were excluded from the angle and depth measurements because of a lack of reference landmarks due to concomitant displaced proximal humeral fractures.

In group D, the RHSL was associated with a lesser tuberosity fracture in 8.8% of the cases and a fracture of the greater tuberosity in none of the cases. In group LD, a fracture of the lesser tuberosity was found in 44.8% of the cases and a fracture of the greater tuberosity in 39.7% of the cases. In the CLD group, a fracture of the lesser tuberosity was noted in 10.0% of the cases and a fracture of the greater tuberosity in 20.0% of the cases. All lesser tuberosity fractures and all but 1 greater tuberosity fractures originated from the RHSL. Posterior glenoid bone loss was observed in 60.0% of all chronic locked dislocations (Table 3).

The 3D reconstructions of available CT scans ( $n = 72$ ) allowed for the measurement of the orientation of the posterior defect margin in relation to the humeral shaft (except for 12 cases with a surgical neck fracture). The mean ( $\pm$ SD) orientation was  $0.3^\circ \pm 8.1^\circ$  of anterior tilt (range,  $-18.9^\circ$  to  $25.1^\circ$ ).

Regarding concomitant soft tissue lesions, the available MRI scans ( $n = 40$ ) revealed a posterior Bankart lesion in 80.0% of the cases, a Pulley lesion in 32.5%, a superior labrum from anterior to posterior (SLAP) lesion in 10.0%, a partial tear of the long head of the biceps tendon in 7.5%, a partial tear of the subscapularis tendon in 12.5%, a complete tear of the subscapularis tendon in 7.5%, and a partial tear of the supraspinatus tendon in 10.0%.

In the D group, 76.5% of the cases were surgically treated by means of various techniques, but only 11.8% of all RHSLs were directly addressed by performing subscapularis remplissage (also called the McLaughlin procedure) (5.9%), arthroscopically assisted defect elevation (2.9%), or a combination of the McLaughlin procedure and bone grafting (2.9%). In group LD, 75.9% of the cases were

TABLE 1  
Characteristics of Patients With Reverse Hill-Sachs Lesions Resulting From Different Types of Posterior Instability

	Dislocation	Locked Dislocation	Chronic Locked Dislocation	P Value
Age, mean ± SD, y	40.3 ± 17.5	50.0 ± 13.9	53.4 ± 14.0	.006
Sex, male/female, %	76/24	88/12	80/20	.347
Dominant side, %	52.9	56.9	60.0	.899
Generalized joint hyperlaxity, %	29.4	1.8	0	<.001
Contralateral instability, %	13.3	19.0	0	.163
Previous stabilization surgery, %	5.9	3.4	0	.674
Multidirectional instability, %	11.8	6.9	0	.439
Recurrent instability, %	44.1	5.2	0	<.001
Time since first instability episode, mean ± SD, y	2.5 ± 6.4	>10.0 <sup>a</sup>	—	—
Time since last instability episode, mean ± SD, d	19.1 ± 31.7	7.3 ± 25.1	103.4 ± 54.3 <sup>b</sup>	<.001

<sup>a</sup>For all 3 patients with recurrence.

<sup>b</sup>One patient with a chronic locked dislocation for 12 years was excluded.

TABLE 2  
Causes for Posterior Instability in Patients With Reverse Hill-Sachs Lesions

Dislocation <sup>a</sup>		Locked Dislocation <sup>a</sup>		Chronic Locked Dislocation	
Cause	%	Cause	%	Cause	%
Fall	24	Fall	34	Fall	40
Other sports	21	Convulsive seizure	29	Convulsive seizure	30
Minor trauma	15	Bicycle accident	14	Bicycle accident	20
Convulsive seizure	15	Skiing accident	10	Electrical accident	10
Bicycle accident	15	Electrical accident	7	Motor vehicle accident	0
Motor vehicle accident	6	Motor vehicle accident	3	Skiing accident	0
Skiing accident	6	Minor trauma	2	Other sports	0
Electrical accident	0	Other sports	0	Minor trauma	0

<sup>a</sup>Percentages do not sum to 100% due to rounding effect.

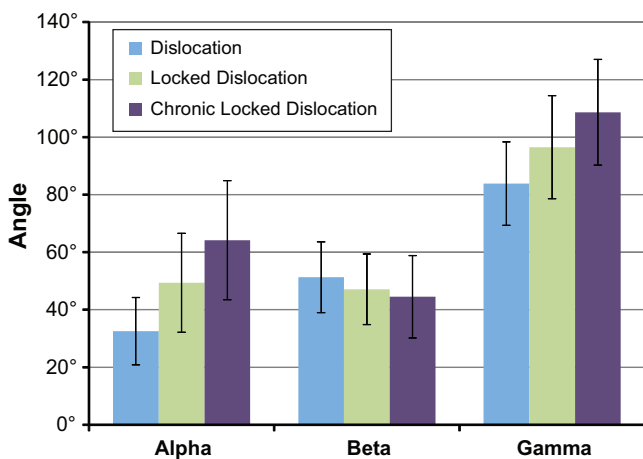


Figure 3. Comparison of the mean alpha angle (defect extent), beta angle (defect localization), and gamma angle (combination of alpha and beta angles) of the 3 different groups of reverse Hill-Sachs lesions.

treated surgically, and 37.9% of the RHSLs were addressed by open or arthroscopic defect elevation (13.8%), hemiarthroplasty (8.6%), the McLaughlin procedure (5.2%), bone grafting of the defect (5.2%), transposition of the lesser

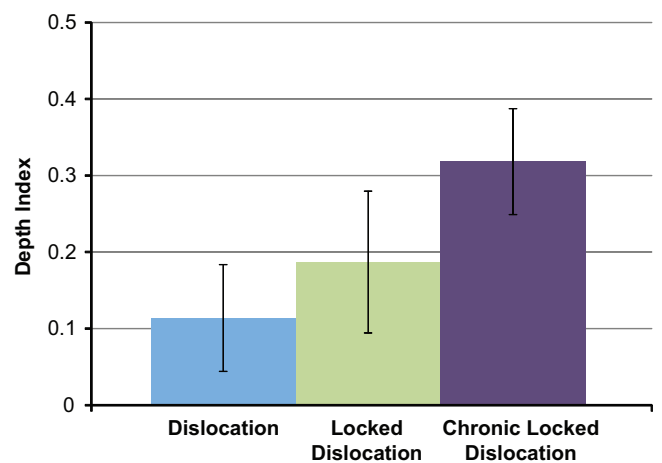


Figure 4. Comparison of the mean depth index of the 3 different groups of reverse Hill-Sachs lesions.

tuberosity into the defect (called the Neer procedure) (3.4%), and rotational osteotomy plus defect elevation (1.7%). In the CLD group, all cases were treated surgically, and the RHSL was addressed in all cases by total arthroplasty (20.0%) or hemiarthroplasty (50.0%), bone grafting

TABLE 3  
Pattern of Concomitant Bony Defects<sup>a</sup>

	Dislocation	Locked Dislocation	Chronic Locked Dislocation
LT fracture	5.9	20.7	0
Displaced LT fracture	2.9	24.1	10.0
LT fractures originating from RHSL	100.0	100.0	100.0
GT fracture	0	19.0	10.0
Displaced GT fracture	0	20.7	10.0
GT fractures originating from RHSL	—	95.7	100.0
Surgical neck fracture	0	20.7	0
Posterior glenoid rim fracture	8.8	5.2	0
Posterior glenoid bone loss	14.7	8.6	60.0

<sup>a</sup>Results are reported as percentages. GT, greater tuberosity; LT, lesser tuberosity; RHSL, reverse Hill-Sachs lesion.

of the defect (10.0%), rotational osteotomy (10.0%), as well as the Neer procedure with additional plating (10.0%).

## DISCUSSION

The goal of this study was to determine the pathomorphological characteristics and patterns of RHSLs in patients after a posterior shoulder dislocation. For this reason, data from a large group of patients with sustained posterior shoulder dislocations and a diagnosed RHSL were gathered in a multicenter study, and defect characteristics in terms of the size, localization, and depth index were determined on CT or MRI scans by means of standardized measurements.

Patients in group D were, on average, significantly younger than patients in group LD and group CLD. Additionally, they had a higher frequency of generalized joint hyperlaxity and a higher proportion of recurrent posterior shoulder instability. Except for the delayed diagnosis and treatment, patients with a CLD-type defect featured similar general characteristics as patients with an LD-type defect. Accordingly, the 3 most common causes of injury in both the LD and CLD groups were simple falls, convulsive seizures, and bicycle accidents. In group D, a considerable proportion of posterior shoulder instability was caused by minor trauma.

While the localization was similar for all 3 groups, defect size and depth significantly increased from group D to group LD to group CLD. Similarly, the gamma angle as a predictor of re-engagement of an RHSL with the posterior glenoid rim increased significantly from group D to group LD to group CLD. In a biomechanical study, the critical gamma angle, above which re-engagement is likely to occur, was identified to be approximately 90°. <sup>9</sup> Therefore, D-type defects seem to be mostly nonengaging, while CLD-type defects are highly likely to re-engage after reduction. LD-type defects feature an intermediate risk of re-engagement, largely depending on their gamma angle and the degree of glenohumeral internal rotation achievable by the patient. In general, it has to be noted that every RHSL must have shown some type of engagement with the posterior glenoid rim during its formation. In the course of posterior instability events, nonphysiological posterior

translation of the humeral head takes place along with forced internal rotation, leading to subluxation or dislocation of the glenohumeral joint and subsequent impaction of the posterior glenoid rim into the humeral head. Once the acute traumatic phase with elongation and possibly damage of the soft tissue stabilizers is past and the glenohumeral joint is reduced, a functioning rotator cuff keeps the joint centered, preventing it from further nonphysiological posterior translation. Therefore, RHSLs with a small gamma angle will not re-engage during rotational movement, while RHSLs with a large gamma angle will keep engaging. Despite the wide variance of treatments for instability recorded for the patients in this study and the current lack of treatment guidelines, the proportion of surgically addressed RHSLs in the 3 different groups corroborates our findings, with only 12% of type D defects being surgically addressed, 38% of type LD defects, and 100% of type CLD defects.

An interesting and previously not described finding was the unexpectedly high number of associated fracture components. A concomitant fracture of the lesser or greater tuberosity was noted more often in the CLD group and especially in the LD group than in the D group, with many of the fractures showing a displacement greater than 5 mm. All of the lesser tuberosity fractures originated from the RHSL. Interestingly, also 96% of the accompanying greater tuberosity fractures originated from the RHSL, creating a head split-type fracture pattern (Figure 5).

In light of the findings of this study and previously published biomechanical tests, we propose the following classification system for RHSLs: type 1 = dislocation (low re-engagement risk); type 2 = locked dislocation (moderate re-engagement risk); and type 3 = chronic locked dislocation (high re-engagement risk) (Figure 6). The distinction between types 1, 2, and 3 based on the pathogenesis and chronicity of the defect is easy to make and helps identify defects prone to re-engagement. While locked dislocations (types 2 and 3) are usually connected to and therefore an indicator for the presence of a large RHSL, nonlocked dislocations (type 1) typically feature smaller RHSLs with a low risk for re-engagement. The distinction between a type 2 and type 3 RHSL is based on the chronicity of the defect, which is an

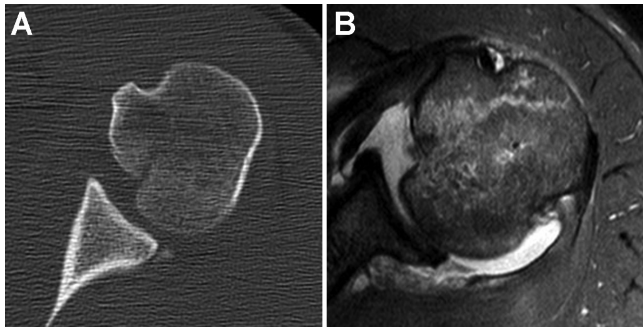


**Figure 5.** (A) Computed tomography (CT) and (B) magnetic resonance imaging (MRI) scans of a reverse Hill-Sachs lesion (RHSL) with a concomitant fracture of the greater tuberosity. The fracture line originates from the RHSL and extends until reaching the lateral cortex of the greater tuberosity. Because of the absence of a dislocation, the fracture is difficult to identify on CT scans but is evident on MRI scans because of the accompanying bone bruise.

important factor to consider when choosing the appropriate treatment. In contrast to acute locked dislocations (type 2) with a typically large defect size but a low rate of posterior glenoid defects, chronic locked dislocations (type 3) typically feature an even larger humeral defect size and a higher rate of posterior glenoid defects, both mostly because of progressive attritional cartilage and bone loss caused by glenohumeral motion in a locked dislocation position. This bipolar bone loss situation creates a high risk for re-engagement as described for Hill-Sachs lesions in anterior shoulder instability.<sup>3,6</sup>

Further predictions of defect re-engagement and therefore the necessity of surgical treatment can be accomplished by measurements of the gamma angle on axial CT or MRI scans, with the critical threshold value being approximately 90°. The nonoperative treatment of small defects has been reported to result in good clinical and acceptable radiological outcomes at midterm follow-up<sup>4,15</sup>; however, especially in young patients, it must be kept in mind that even non-re-engaging small anterior defects will articulate with the glenoid surface during internal rotation, potentially increasing the long-term risk for early-onset osteoarthritis.<sup>8,9</sup> On the contrary, in elderly patients, even larger defects with gamma angles slightly above 90° will not re-engage because of the natural restriction of range of motion in internal rotation.

**Limitations**

Because of the multicenter study design, the available CT and MRI scans differed in quality; however, RHSLs represent a fairly rare injury, and only the collaboration of multiple high-volume shoulder departments collecting their cases over a time span of 10 years allowed us to build a database of over 100 cases, which, to our knowledge, is by far the largest case collection of RHSLs available at this time point.

	Type	Re-engagement risk
Dislocation	1	low
Locked Dislocation	2	moderate
Chronic Locked Dislocation	3	high

**Figure 6.** Classification of reverse Hill-Sachs lesions.

Measuring the defect extent and localization in the coronal plane was attempted but could not be sufficiently accomplished because of the often far anterior localization of the defects, which then were insufficiently displayed in the coronal imaging planes. Even so, the transverse plane appears sufficient to analyze the extent and localization of defects relevant for engagement because their posterior defect margin is aligned approximately parallel to the humeral shaft axis and engagement with the posterior glenoid rim occurs accordingly during internal rotation with the arm in an otherwise neutral position.<sup>9</sup> Even though, in the literature, posterior shoulder dislocations are often ascribed to an axial force exerted on the arm in flexion, adduction, and internal rotation,<sup>8</sup> evidence on the subject is scarce, and the defect orientation suggests that at the time of impaction of the humeral head, the arm is internally rotated but not necessarily flexed. This might also explain why patients with a locked posterior dislocation usually have their arm fixed in mere internal rotation without significant flexion or extension.

A limitation of this study is the lack of CT scans and 3D reconstructions of the glenoid in many cases, which prevented the exact measurement of posterior glenoid defects. Nonetheless, defects could be identified in the form of posterior glenoid rim fractures in acute instability cases and the loss of posterior glenoid rim contour in chronic cases with attritional bone loss or fracture fragment resorption.

**CONCLUSION**

The distinction between the 3 different RHSL types based on the pathogenesis and chronicity of the defect helps identify defects prone to re-engagement. The gamma angle as a measurement of the position of the posterior defect margin and therefore a predictor of re-engagement varies significantly between the defect types. While nonlocked dislocations typically feature RHSLs (type 1) with smaller gamma angles and therefore a low risk for re-engagement, locked dislocations are usually connected to the presence of large RHSLs (type 2) with higher gamma angles and therefore a higher risk of re-engagement. Chronic locked dislocations are typically associated with very large RHSLs (type 3) with the highest gamma angles and concomitant posterior glenoid defects due to attritional bone loss, creating a bipolar bone loss situation with the highest risk for re-engagement.

## ACKNOWLEDGMENT

The authors thank Robert Bogner, Petra Magosch, and Alexander Auffarth for their help with data collection.

## REFERENCES

1. Bogner R, Hubner C, Matis N, Auffarth A, Lederer S, Resch H. Minimally-invasive treatment of three- and four-part fractures of the proximal humerus in elderly patients. *J Bone Joint Surg Br.* 2008;90(12):1602-1607.
2. Cicak N. Posterior dislocation of the shoulder. *J Bone Joint Surg Br.* 2004;86(3):324-332.
3. Di Giacomo G, Itoi E, Burkhart SS. Evolving concept of bipolar bone loss and the Hill-Sachs lesion: from "engaging/non-engaging" lesion to "on-track/off-track" lesion. *Arthroscopy.* 2014;30(1):90-98.
4. Duralde XA, Fogle EF. The success of closed reduction in acute locked posterior fracture-dislocations of the shoulder. *J Shoulder Elbow Surg.* 2006;15(6):701-706.
5. Green A, Izzi J Jr. Isolated fractures of the greater tuberosity of the proximal humerus. *J Shoulder Elbow Surg.* 2003;12(6):641-649.
6. Hedtmann A, Kircher J. Instabilitaet des Glenohumeralgelenks. *Obere Extremitaet.* 2014;9(2):68-77.
7. Hill HA, Sachs MD. The grooved defect of the humeral head: a frequently unrecognized complication of dislocations of the shoulder joint. *Radiology.* 1940;35:690-700.
8. Kowalsky MS, Levine WN. Traumatic posterior glenohumeral dislocation: classification, pathoanatomy, diagnosis, and treatment. *Orthop Clin North Am.* 2008;39(4):519-533, viii.
9. Moroder P, Runer A, Kraemer M, et al. Influence of defect size and localization on the engagement of reverse Hill-Sachs lesions. *Am J Sports Med.* 2015;43(3):542-548.
10. Moroder P, Tauber M, Hoffelner T, et al. Reliability of a new standardized measurement technique for reverse Hill-Sachs lesions in posterior shoulder dislocations. *Arthroscopy.* 2013;29(3):478-484.
11. Paul J, Buchmann S, Beitzel K, Solovyova O, Imhoff AB. Posterior shoulder dislocation: systematic review and treatment algorithm. *Arthroscopy.* 2011;27(11):1562-1572.
12. Rouleau DM, Hebert-Davies J. Incidence of associated injury in posterior shoulder dislocation: systematic review of the literature. *J Orthop Trauma.* 2012;26(4):246-251.
13. Rowe CR, Zarins B. Chronic unreduced dislocations of the shoulder. *J Bone Joint Surg Am.* 1982;64(4):494-505.
14. Saupe N, White LM, Bleakney R, et al. Acute traumatic posterior shoulder dislocation: MR findings. *Radiology.* 2008;248(1):185-193.
15. Wolke J, Kruger D, Gerhardt C, Scheibel M. [Conservative therapy of acute locked posterior shoulder dislocation: clinical and radiological long-term results]. *Unfallchirurg.* 2014;117(12):1118-1124.